Krzysztof Grudzień*, Maciej Niedostatkiewicz**,
Laurent Babout*, Jerome Adrien***

Application of Particle Image Velocimetry Method for Monitoring the Volume Changes during Silo Flow on the Basis of X-Radiographs

1. Introduction

Main reasons influencing on stability of the silo is non-symmetrical flow of the bulk solid and non-controlled volume changes in the hopper [20]. Both of them are connected with the shape and the dimension of the core of flow, created from the beginning of silo emptying process. Knowledge about the flow profile and mechanism of concentration changes, also at the core of flow allows to protect silo from the damage. This problem is very crucial in case of silos with funnel flow. Due to discrete character of the granular materials stored in the silo monitoring of the volume changes needs to application of the non-invasive methods to describe their behaviour.

X-ray radiation is one of the non-invasive measurements methods which can be apply for monitoring the concentration changes in bulk solid. Earlier it was used not only for monitoring the bulk solid flow in the silo [1, 9, 12], but also during other geotechnical tests [6, 21]. X-ray method allows describe qualitatively the area of volume changes and also monitoring the thickness of the shear zone along the silo walls and inside the bulk solid, which influence of silo wall pressure. Till now mainly separate exposure of the X-ray radiation was used for monitoring the concentration changes during deformation process of the bulk solid. X-ray tomography allows for 3D measurement of concentration changes during granular material deformation.

Particle Image Velocimetry (PIV) method is based on the numerical analysis of successive pairs of digital photographs of the side of deformed specimen. PIV measurement method was used with success for silo flow analysis [14, 15, 18] and similarly to X-ray radiation it was also used for different geotechnical tests [13, 22].

* Computer Engineering Department, Technical University of Lodz, Poland
** Faculty of Civil and Environmental Engineering, University of Lodz, Poland
*** Université de Lyon, MATEIS CNRS, Villeurbanne, France

The main intentions of the paper are following:

1) to show the potential PIV methods to quantitatively measure volume changes at the core of flow in dry sand during funnel silo flow and
2) trial of PIV correlation performed on the basis of the X-ray tomography measurements. The comparison of volume changes by X-rays with corresponding results by PIV in the same model silo calculated on the basis of measured displacements on the sand surface,
3) application of the PIV method for analysis the deformation of the bulk solid during silo emptying using X-ray radiographs received from tests with continuous exposure.

The experiments in model silo were carried out with different initial densities of sand (loose and dense) and silo wall roughness (smooth and very rough wall and hopper). During experiments continuous X-ray exposure for monitoring volume changes in a bulk solid during silo flow was applied. Analysis of radiography allows to gather the additional information about the volume changes, especially in the core of flow and over the outlet. Results were presented as a volumetric strain changes for selected time parts of silo emptying.

2. Measurement method

2.1. X-ray tomography technique

The entire procedure of measurements during silo flow using X-ray tomography can be summarized in 7 steps:

1. specimen placement,
2. choice of radiation parameters,
3. fitting of external filter,
4. time integration of detector,
5. calibration procedure,
6. direct measurement,
7. post-processing data handling and visualization.

The X-radiographs contain the information about the X-ray intensity reduction inside the object. The transmission tomography with a 2D flat panel detector delivers a 2D map of a linear attenuation coefficient μ. The attenuation value from X-radiographs informs about the absorption of X-ray caused by the presence of a specimen between a source and detector. A linear attenuation coefficient for silo walls is constant and is the same for any stage of silo discharge. For a quantitative analysis of the sand behaviour in a silo, it is necessary to conduct a comparison of attenuation coefficient changes at different silo locations. In paper [4] is described method which eliminate the influence of silo wall on later radiographs analysis. After proposed method of data processing (normalization data), the obtained X-radiographs show the values of the absorption coefficient (an inverse of X-ray intensities detected on a sensor and on source radiographs). The value range of new I' intensity is among

(0–1), where the pixel value '0' represents the minimum absorption coefficient (minimum sand concentration – empty silo) and the value '1' the maximum absorption coefficient (maximum sand concentration – filled silo). Thus, the changes of intensity values I' in the range (0–1) represent X-ray absorption coefficient changes depending on the sand concentration. A decrease of the intensity I' means a decrease of the X-ray absorption coefficient (volume increase – sand dilatancy), an increase of the intensity I' means a volume decrease (sand contractancy). For PIV analysis methods was applied radiographs without correction.

2.2. Particle Image Velocimetry (PIV) technique

The entire procedure of measurements during silo flow using PIV can be summarized in 6 steps:

1. subdivide the image into interrogation cells,
2. calculate the image intensity fields at time t and $t + \Delta t$ for one interrogation cell,
3. calculate the correlation between image intensity fields (the most likely displacement is the peak of the function),
4. repeat the procedure for each interrogation cell,
5. convert the Eulerian deformation field into Lagrangian deformation field,
6. calculate strain tensor.

The strain vector is calculated with a strain-displacement matrix used in the finite element method. The volumetric ε_v and deviatoric ε_p strain are presented in equation (1):

$$\varepsilon_v = \varepsilon_{11} + \varepsilon_{22} \text{ and } \varepsilon_p = \sqrt{\varepsilon_{ij}^* \varepsilon_{ij}^*} \text{ with } \varepsilon^* = \varepsilon_{ij} - \frac{1}{3}\varepsilon_{kk}\delta_{ij} \tag{1}$$

where:

ε – deformation vector,
ε_{ij} – deformation tensor,
δ_{ij} – Kronecker deltas.

3. Experimental set-up

3.1. Silo and bulk solid material parameters

The model tests with application of X-ray radiation and PIV method were carried out with rectangular perspex symmetric funnel flow model silo consisting of a bin and a hopper. The height of a funnel flow silo was h = 0.29 m, the width b = 0.15 m, the depth d = 0.07 m (Fig. 1). The width of the rectangular outlet along the silo depth was 5 mm. The wall thickness was 0.005 m. Smooth and very rough walls in a bin and a hopper were used. A wall surface with a high roughness r_w was obtained by sticking a sand paper to the interior wall surfaces ($r_w \approx d_{50}$). The tests were performed with a dry cohesionless sand with a mean grain diameter of d_{50} = 0.8 mm and uniformity coefficient U = 5. An initially loose sand

(unit weight $\gamma = 14.5$ kN/m^3, initial void ratio $e_o = 0.80$) was obtained by filling the silo from a pipe located directly above the upper sand surface which was vertically lifted during filling. An initially dense sand ($\gamma = 17.5$ kN/m^3, $e_o = 0.55$) was obtained by filling the silo using a so-called "rain method" (through a vertically movable sieve located always 250 mm above the top of the silo.

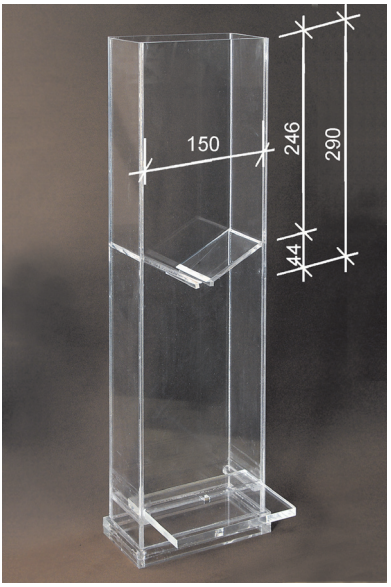

Fig. 1. Rectangular perspex silo model used for funnel flow (dimensions in mm)

3.2. X-ray tomography equipment

During measurement campaign tomograph produced by Phoenix® company was used. Detector (PaxScan 2520V, PaxScan™) in form of silicon flat panel was used, composed of 1920 rows and 1500 lines of sensitive pixels, the size of each is 127 x 127 μm^2. It was used in a 2×2 binning mode. The X-ray source (cone beam) was an open transmission nanofocus X ray tube operated between 40 and 160 kV. In order to receive 3D image the investigated sample was rotated in specimen. Distance between source and detectors during measurement was establish 0.5776 m.

The main parameters chosen before measurement are:

1) geometrical parameters:
   a) focus-object-distance = 341.10 mm,
   b) focus-detector-distance = 577.60 mm,
   c) magnification 1.69,

2) detectors parameters:
   a) detector readout time (acquisition time for one projection)-exposition time: 100 ms,
   b) number of images to be integrated: 10,
   c) number of calibration projections: 50,
   d) detector pixel size: $x = 0.254$ μm, $y = 0.254$ μm,
   e) number of pixels in radiographs: $x = 960$, $y = 768$,
3) source parameters – X-ray tube parameters:
   a) voltage: 145 kV,
   b) current: 180 μA,
   c) dimension of focal spot 4 μm.

In order to reduce beam hardening it was additionally used hardware filtering by placing a filter on the X-ray tube output a thin copper (0.3 mm) plate. The low energy X-rays are absorbed before the beam reaches the material. The received data from detectors were corrected by applied two point calibration methods. For this calculations were used data from offset and gain correction. The results of these procedures is the 2D X-radiographs image in form of 16-bits*.tiff files, which were processed to obtain information about concentration changes during gravitational flow of sand. Details about the X-ray tomography used during experiments are presented in [5].

3.3. Particle Image Velocimetry (PIV) equipment

During experiments industrial digital foto camera with resolution of 1280×960 pixels was used. Images were recorded in *.bmp format in grayscale. The dimension of the AOI (area of interest) was chosen experimentally, equal to ≈0.15×0.2 m^2. Interrogation cell was fixed as a area 64×64 pixels with the displacement of the middle on the first and second images with 12 pixels. Images were recorded in constant form during whole time of silo emptying with the frequency of 40 frames per second ($\Delta t = 0.025$ s). The camera was fixed at a distance of $s = 0.4$ m from the silo model with the axis oriented perpendicular to the plane of deformation. To reduce a shadow effect, two 500-watt flashes were used for continuous illumination. The flashes were situated at distance of 1.0 m from the silo under the angle of 45^o. No polarization filter was used for the camera.

The accuracy of the PIV method for application at the granular flow was discussed in [15, 22]. Details about application of PIV for silo flow were presented in [18].

Results presented in this paper were performed using the program *GeoPIV*, elaborated in [15, 22], used to determine displacements and strains in sand. It is a MatLab module which implements Particle Image Velocimetry (PIV) in a manner suited to 2D geotechnical testing, which runs at the MatLab command line. Accuracy of the *GeoPIV* in aspect to another commercial PIV programs was discussed in [11].

4. Experimental results

Tests were performed in 5 steps:

1) in *1st step* experiments with colored grain were performed-the intention of the tests was to observe the formation of the core of flow for different initial conditions,
2) in *2nd step* experiments with application of X-ray radiation were performed-the target of one was to observed the spatial volume changed at the core of flow,
3) in *3rd step* experiments with application of the PIV measurement technique were performed-the intention of tests was to observe changes of the volumetric strain at the next to the transparent wall part of the silo,
4) in *4th step* direct comparison of volume changes by X-rays (*2nd step*) with corresponding results by PIV (*3rd step*) were performed,
5) in *5th step* received earlier radiographs (*2nd step*) were analysed using PIV technique (used earlier at the *3rd step*)-the target of one was to receive some more information about the volume changes at the core of flow due to fact that correlated images (radiographs) consist spatial information about the volume changes.

In case of experiments with X-radiation and PIV the same methods of filling were used. The sand paper used to increase the wall roughness was also the same.

4.1. Displacement in sand

In case of experiments with loose sand and smooth walls localization in form of shear zone along the walls at the bin were not observed due to creation of the dead zone (stagnant zone). The width of the core of the flow, which appeared from the beginning of the silo opening increased from the 65 mm ($81 \times d_{50}$) at the initial state to 107 mm ($134 \times d_{50}$) at the advanced flow (Fig. 2a). The flow was symmetrical.

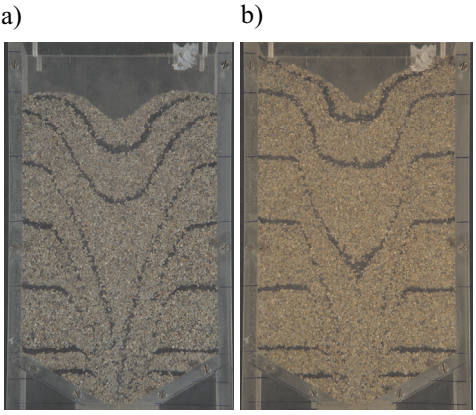

Fig. 2. Displacement in: a) loose; b) dense sand $d_{50} = 0.8$ mm after 8 s of emptying rectangular silo with funnel flow (smooth walls, gravitational flow)

Increasing of the initial density not influence on the type of flow. Localization along the bin walls were not noticed, similarly to tests with loose sand. The width of the core of the flow decreased-from the 56 mm ($70\times d_{50}$) at the initial state to 100 mm ($125\times d_{50}$) at the advanced flow (Fig. 2b). The flow also was symmetrical.

Increasing of the wall roughness significantly not influence at the flow profile. The width of the core of flow decreased ≈2 mm ($2.5\times d_{50}$) during tests with loose sand and ~3 mm ($4\times d_{50}$) during tests with dense one.

4.2. X-ray tomography measurement

On Figure 3 is presented position of horizontal cross-section profiles along silo height used during the sequences of X-radiographs analysis for different initially packing density of sand and smooth and rough silo wall.

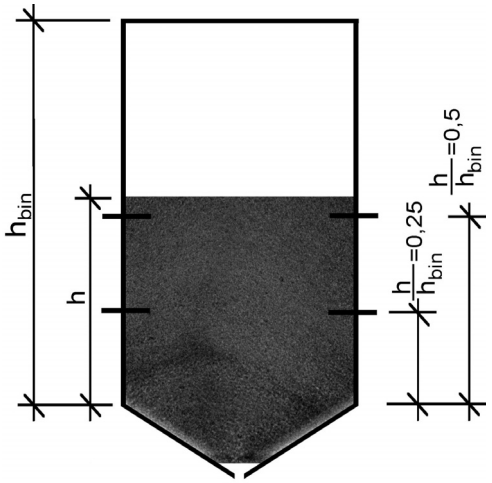

Fig. 3. Position of the horizontal cross-sectional profiles along the silo height used during X-ray tomography experiments (h – height above the transition between hopper and bin, h_{bin} – height of the parallel (vertical) part of the silo)

In case of experiments with loose sand and smooth walls creation of the core of flow was observed just from the beginning of silo emptying. The width of the core of flow changed dynamically-increased from the 70 mm ($88\times d_{50}$) at the initial state to 110 mm ($138\times d_{50}$) at the advanced flow (Fig. 4Aa). At the end of emptying of the silo the angle of inclination of the stagnant zone was ≈60°. The localizations along the bin walls and also parabolic dilatants zones inside the core of low were not observed. During experiments with dense sand and smooth walls core of flow appeared as in case of test with loose sand-after start of silo discharging. The width of the core of flow was narrower-increased from the

45 mm ($57\times d_{50}$) at the initial state to 100 mm ($125\times d_{50}$) at the advanced flow (Fig. 4Ab). At the end of emptying of the silo the angle of inclination of the stagnant zone was ≈85°. The localizations along the bin walls did not appeared.

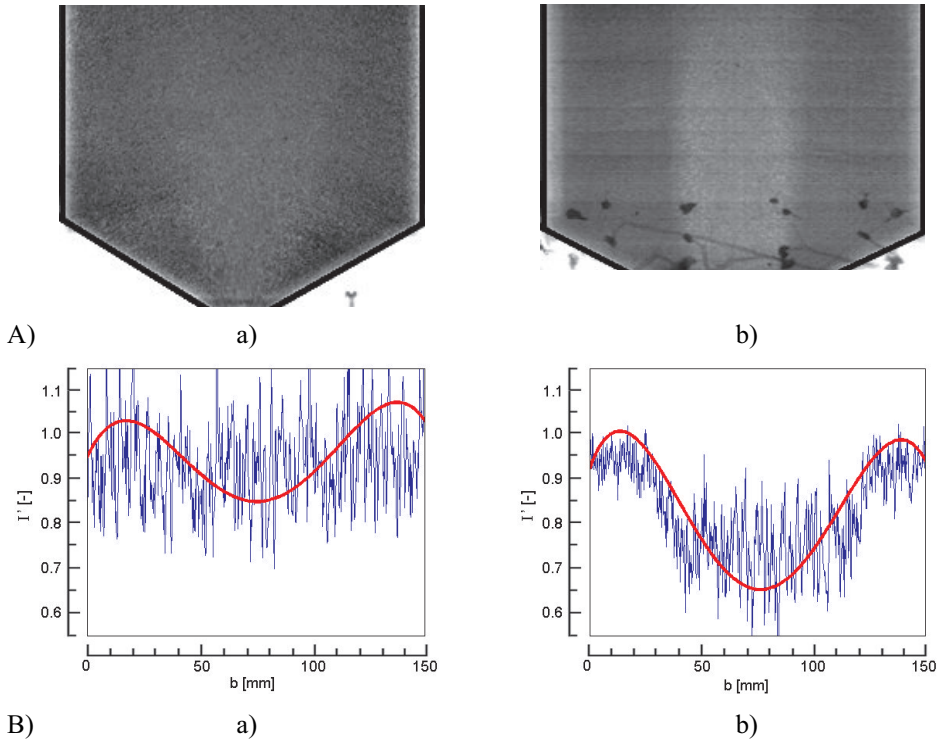

Fig. 4. X-ray radiographs (A) and 1D visualization (B) after 6 s of emptying rectangular silo with funnel flow at bin height $h/h_{bin} = 0.25$ on the basis of X-rays (expressed by pixel normalized intensity I'): a) loose sand, smooth walls; b) dense sand, smooth walls (h – height above the transition between hopper and bin) (>1.0 – volume increase (contractancy), <1.0 – volume decrease (dilatancy), ← – discharge beginning) ($d_{50} = 0.8$ mm, gravitational flow), b – the width

In case of experiments with loose sand and very rough walls creation of the core of flow was observed just from the beginning of silo emptying. The width of the core of flow changed rapidly- from the 65 mm ($81\times d_{50}$) (initial state) to 105 mm ($132\times d_{50}$) (advanced flow) (Fig. 5Aa). At the end of emptying of the silo the angle of inclination of the stagnant zone was ≈65°. Due to presence of one the sand did not moved along the bin walls.

During experiments with dense sand and very rough walls core of flow appeared as in case of test with loose sand-after start of silo discharging. The width of the core of flow was narrower-increased from the 40 mm ($50\times d_{50}$) (initial state) to 90 mm ($113\times d_{50}$) (advanced flow) (Fig. 5Ab). At the end of emptying of the silo the angle of inclination of the stagnant

zone was ≈85°. The flow was non-symetrical, internal parabolic localization inside the flowing sand at the core of flow were not observed.

The stagnant zone was more clear visible in case of experiments with dense sand (Fig. 4Bb, 5Bb) than loose sand. During experiments with dense sand and very rough walls contractancy at the area of stagnant zone was steady and uniform, equal to ≈15% of the initial state, at the core of flow dilatancy was ≈30% of the value of the initial state. During experiments with dense sand and smooth walls contractancy at the area of stagnant zone was up to ≈8% of the initial state. At the core of flow dilatancy was ≈35% of the value of the initial state. In case of loose sand and very rough walls contractancy ≈12% of the value of the initial state took place at the stagnant zone, at the core of flow dilatancy was ≈25% of the value of the initial state, similar to experiments with loose sand and smooth walls.

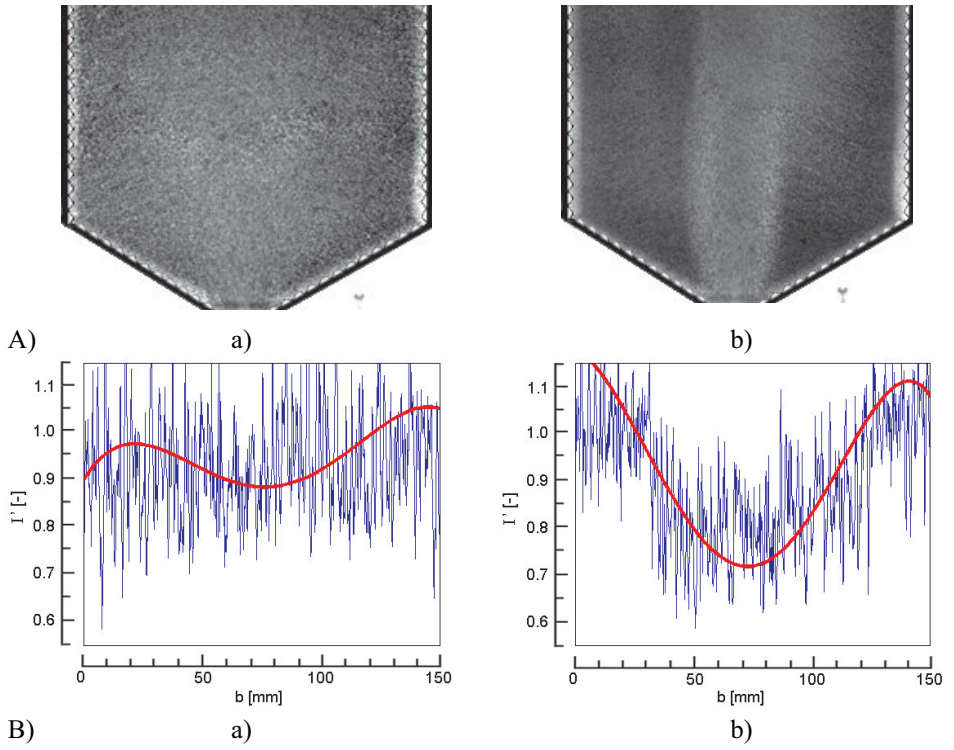

Fig. 5. X-ray radiographs (A) and 1D visualization (B) after 6 s of emptying rectangular silo with funnel flow at bin height $h/h_{bin} = 0.25$ on the basis of X-rays (expressed by pixel normalized intensity I'): a) loose sand, very rough walls; b) dense sand, very rough walls (h – height above the transition between hopper and bin) ($d_{50} = 0.8$ mm, gravitational flow)

The width of the core of flow during experiments with dense sand was the same for smooth and very rough walls. The similarity was observed both at the height of the bin 0.25 and 0.5.

4.3. Particle Image Velocimetry (PIV) measurement

During experiments both deviatoric ε_p and volumentric ε_v strain were calculated, in the paper only the last one are presented (due to similarity of the volume changes observed on radiographs). The magnitude of contractancy (volume decrease) is denoted by numbers with the sign (+) and dilatancy (volume increase) is described by numbers with the sign (–). The colour scale division is similar with initially loose and dense sand, independly of the wall roughness.

During experiments with loose sand and smooth walls any localization along the bin walls were not observed (Fig. 6a). Shear zones were created along the flow core edges-contractancy on the basis of ε_v between the core of flow and stagnat zones was observed. Also at the lower part of the silo the contractancy appeared. Distribution of the volumetric strain ε_v at the core of flow was non-uniform. The width of the core of flow changed-at the advanced flow increased to 108 mm ($135 \times d_{50}$). The angle of inclination of the stagnant zone was $\approx 58^{o}$. The flow was slightly non-symetrical. At h/h_{bin} = 0.25 at the 6 s of silo emptying at the core of flow dilatancy was ≈15% of the value of the initial state.

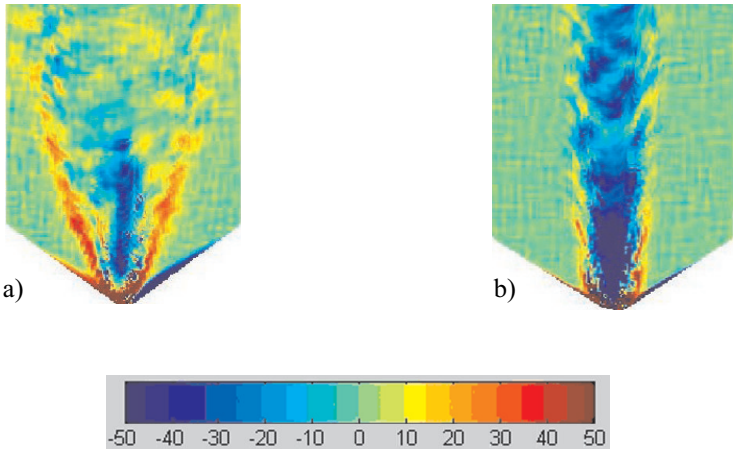

Fig. 6. Evolution of the volumetric strain ε_v in sand d_{50} = 0.8 mm after 6 s of emptying rectangular silo with funnel flow: a) loose sand, smooth walls; b) dense sand, smooth walls (gravitational flow) (on the basis of the digital images)

In case of experiments with dense sand and smooth walls rapid dilatancy at the core of flow appeared at the beginning of silo emptying (Fig. 6b). Contractancy took place over the outlet, along the core of flow. Non-uniformity volumetric strains ε_v at the core of flow was registred. The width of the core of flow got value of 80 mm ($100 \times d_{50}$) (advanced flow), due to the angle of inclination of the stagnant zone $\approx 82^{o}$. At h/h_{bin} = 0.25 at the 6 s of silo emptying at the core of flow dilatancy was ≈31% of the value of the initial state.

During experiments with loose sand and very rough walls volumetric strains ε_v observed in the sand were similar to one during experiment with smooth walls (Fig. 7a). On

the basis of volumetric starin ε_v contractancy along the flow core edges and at the lower part of the silo were obserwed. Distribution of the volumetric strain ε_v at the core of flow was non-uniform. Increasing of the wall roughness not influenced on the width of the core of flow-either at the initial state of flow or during advanced flow. Dilatancy at the core of low was equal to one during tests with loose sand and smooth walls.

In case of experiments with dense sand and very rough walls sand flowed similary to one during test with smooth walls (Fig. 7b). Not only the non-uniformity of the core of flow was noticed, but also the lack of symmetry of flow appeared. The width of the core of flow was similar to observed during test with smooth walls. The dilatancy was also at the same range as in case of tests with smooth walls.

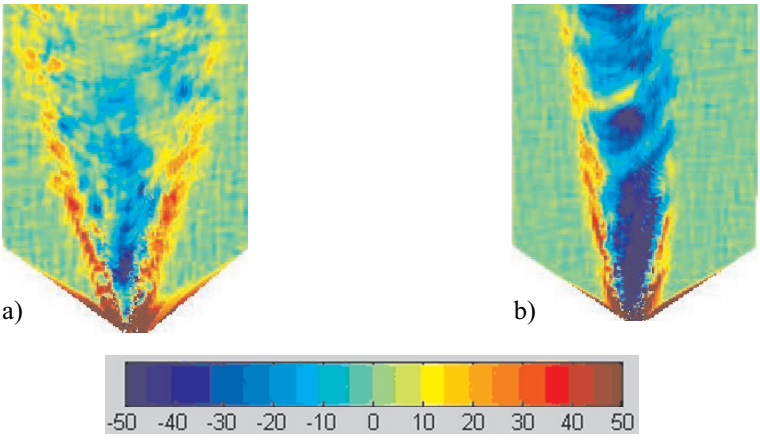

Fig. 7. Evolution of the volumetric strain ε_v in sand $d_{50} = 0.8$ mm after 6 s of emptying rectangular silo with funnel flow: a) loose sand, very rough walls; b) dense sand, very rough walls (gravitational flow) (on the basis of the digital images)

The results from both methods show the same evolution tendency of volume changes. Similar agreement at the tendency was observed during experiments both with loose and dense sand, independly of the wall roughness (due to similarity in the paper the comparisons of the results for smooth walls are presented). Both methods (X-ray and PIV) show the tendency to dilatancy at the core of flow. On the basis of received results we can conclude that the X-ray method provides larger volume changes. The differences are probably caused by the fact that volume changes in PIV were determined on the specimen surface (under friction). In turn, volume changes by X-rays were calculated from a certain relatively large volume by taking into account the silo depth.

4.4. Particle Image Velocimetry (PIV) measurement on the basis of the X-ray tomography measurement

The radiographs received from tomography measurement were additionally tested with PIV method. The idea of the correlation of the next to one radiographs using PIV method

was to find additional information called spatial information not possible to receive in case of analysing the digital images of the displacement of the sand at the transparent silo wall [10].

In case of results for test with loose sand and smooth walls the non-uniformity of core was observed (Fig. 8a). Additionally the formation of the semi-arches at the core of flow was observed which collapsed during the advanced flow. Interesting situation was observed during tests with dense sand and smooth walls, loose and dense sand during tests with very rough walls (Figs. 8b and 9ab). The situation was observed in the strongest form in case of experiment with dense sand and smooth walls (Fig. 8b). Contractancy observed on the basis of the volumetric strain ε_v took place in the middle of the dilatants core of flow.

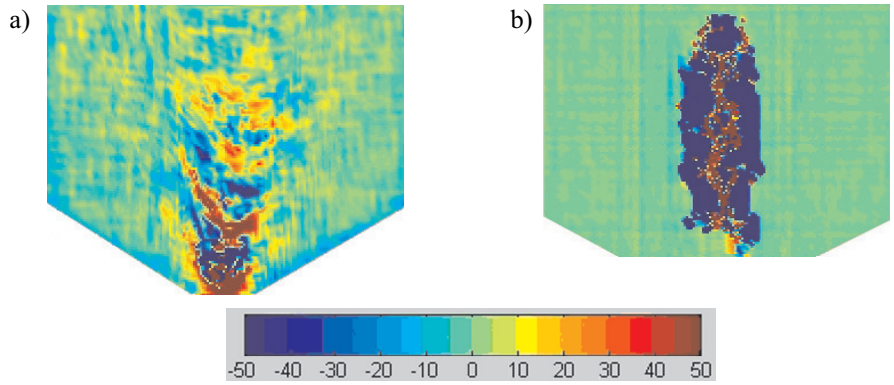

Fig. 8. Evolution of the volumetric strain ε_v in sand d_{50} = 0.8 mm after 6 s of emptying rectangular silo with funnel flow: a) loose sand, smooth walls; b) dense sand, smooth walls (gravitational flow) (on the basis of the X-radiographs)

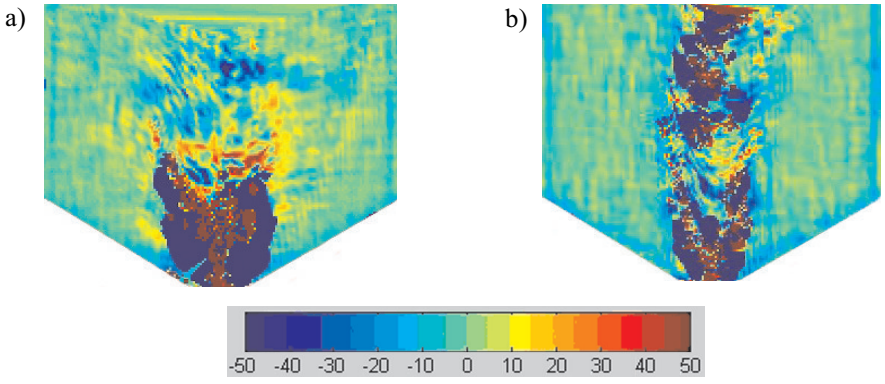

Fig. 9. Evolution of the volumetric strain ε_v in sand d_{50} = 0.8 mm after 6 s of emptying rectangular silo with funnel flow: a) loose sand, very rough walls; b) dense sand, very rough walls (gravitational flow) (on the basis of the X-radiographs)

The exploitation of the appearance of the contractancy at the central part of the core of flow are following:

1) mistakes of the PIV method correlation,
2) circular oscillation at the core of flow discover due to fact the radiographs include information about the spatial volume changes.

According to the first reason X-ray images were performed with lower resolution (960×768) compare to images received from digital photos (1280×960). Also the time interval was higher (0.1 s to 0.025 s). Above situation could cause that contractancy observed at the central part of the flowing material is form of artefact as a result of the lack of correlation-the grain at the central part of silo flow with high speed so the correlation at this profile is only stochastically, not real. The reason of the results as a correlation problems looks with very strong basement. To confirm this theory is worth mansion that local contractancy at the central part of the silo appeared also at the hopper in case of experiments with mass flow silo (Fig. 10) – contractancy was not observed during classical PIV experiments (Fig. 11), but were registered during trial of correlation of the X-ray radiographs (Fig. 12). According to the second reason during flow local oscillation at the low part of the silo appeared. Turbulents and oscillations in the granular materials, not only at the silos, were the subject matter of analysis for many years [8]. This problem was simulated with numerical models [7, 24]. The similarity of the turbulent flow of the bulk solid to flow of the water thru the outlet was suggested in [19]. They pointed, that this type of phenomenon could be appear during silo emptying process as three-dimensional formation of local volume increase. Is worth thinking if observed contractancy is the circumferential oscillation of the sand which appeared during the silo emptying. This type of formation of flow can be compare to water flow thru the circular outlet, due to conception about the similarity of flow of bulk solid and the water near the outlet formulated earlier in [19]. The weak part of this theory is that outlet is not circular but strip (along the whole deep of the silo).

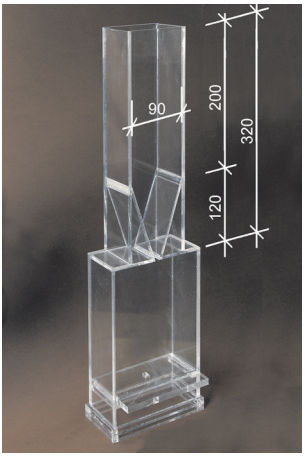

Fig. 10. Rectangular perspex silo model used for mass flow (dimensions in mm)

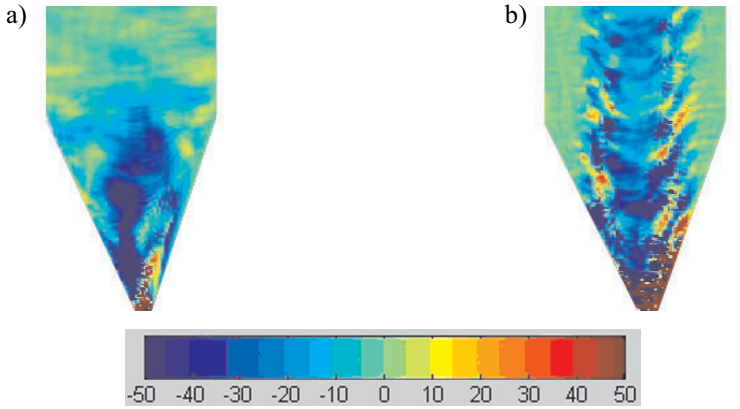

Fig. 11. Evolution of the volumetric strain ε_v in sand $d_{50} = 0.8$ mm after 3 s of emptying rectangular silo with mass flow: a) dense sand, smooth walls; b) dense sand, very rough walls (gravitational flow) (on the basis of the digital images)

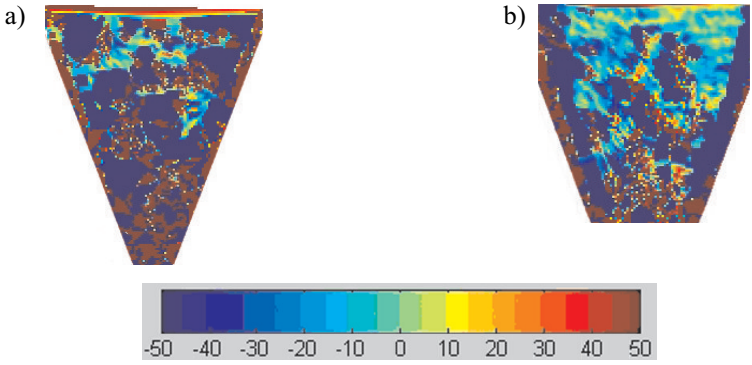

Fig. 12. Evolution of the volumetric strain ε_v in sand $d_{50} = 0.8$ mm after 3 s of emptying rectangular silo with mass flow: a) dense sand, smooth walls; b) dense sand, very rough walls (gravitational flow) (on the basis of the X-radiographs)

5. Conclusions

The Particle Image Velocimetry (PIV) method can be used as a non-invasive optical technique to measure deformations on the surface of granular materials on the basis of processing successive digital images performed without any physical contact. During emptying funnel flow silo the wall roughness did not influence the flow kinematics. The distribution of volumetric strain was non-uniform in the flow core independently of the initially density, the shape of the flow core was symmetric for loose sand only. The core width increased with increasing initial sand density. Dilatancy occurred mainly in the flow

core. Contractant shear zones were created at the flow core edges during experiment with loose sand.

Application of the X-ray radiation with continuous exposure on the basis of the X-ray tomography allows for monitoring the bulk solid concentration during silo emptying. At the stagnant zones, along the silo walls at the bin contractancy of the bulk solid was mainly observed on the basis of the light intensity function. The width of the core of flow was similar to one performed using PIV measurement technique. Frequency of the radiation with 10 frames per second is enough to quantitatively description both of concentration changes and localization formation at flowing sand.

Connection of X-radiation with continuous exposure and correlation of the radiographs using PIV method allows to detect unexpected contractancy at the core of flow. Lack of correlation between radiograph and low resolution of the images are probably the major reasons of the mistakes.

The experiments will be continued to solve the problem of the creation of the local contractancy a the core of flow. Tests with cylindrical model silo equipment with circular outlet will be performed. X-ray tomography with higher frequency of registration of the frames will be used.

Acknowledgements

The work is funded by the European Community's Sixth Framework Programme – Marie Curie Transfer of Knowledge Action (DENIDIA, contract No.: MTKD-CT-2006-039546). The work reflects only the author's views and the European Community is not liable for any use that may be made of the information contained therein.

K. Grudzien is a scholarship holder of project entitled „Innovative education" supported by European Social Fund.

References

[1] Blair-Fish P., Bransby P.L., *Flow pattern and wall stresses in a mass-flow bunker*. J. Eng. Ind. Trans. ASME, B 95, 1, 1973, 17–26.

[2] Buffičre J.-Y., Cloetens P., Ludwig P., Maire E., Salvo L., *In Situ X-Ray tomography studies of microstructural evolution combined with 3D modelling*. MRS Bulletin, 33, 2008.

[3] Fischer F., Hoppe D., Schleicher E., Mattausch G., Flaske H., Bartel R., Hampel U., *An ultra fast electron beam x-ray tomography scanner*. Meas. Sci. Technol., 19, 2008.

[4] Grudzień K., Niedostatkiewicz M., Adrien J., Maire E., Sankowski D., *Quantitatively description of the bulk solid concentration changes based on X-ray continuous radiation*. Proc. of the 6th World Congress on Industrial Process Tomography, China, 2010 (accepted).

[5] Grudzień K., Niedostatkiewicz M., Adrien J., Tejchman, J., Sankowski D., *Quantitative estimation of volume changes of granular materials during silo flow using X-ray tomography*. Chemical Engineering and Processing, 2010 (under opinion).

[6] Leśniewska D., Muir Wood D., *Observations of stresses and strains in a granular material*. Journal of Engineering Mechanics, 2009 (in print).

[7] Liu S., Xiang X., Luo Q., *Theoretical analysis and numerical simulation of turbulent flow around sand waves and sand bars*. Journal of Hydrodynamics, B21, 2, 122, 2009, 292–298.
[8] Mathieu J., Scott J., *An introduction to turbulent flow*. Cambridge University Press, 2000.
[9] Michalowski R.L., *Flow of granular material through a plane Hopper*. Powder Technology, 39, 1984, 29–40.
[10] Niedostatkiewicz M., Grudzień K., Sankowski D., *Measurement of volume changes in the silo on the basis of the X-ray radiographs using PIV technique*. Proc. of the 6th World Congress on Industrial Process Tomography (WCIPT-6), Pekin, 2010 (under opinion).
[11] Niedostatkiewicz M., Leśniewska D., Tejchman J., *Experimental analysis of shear zone patterns in sand for earth pressure problems using Particle Image Velocimetry.* Strain, 2010 (in print).
[12] Niedostatkiewicz M., *Application of x-ray technique for monitoring deformation of granular materials*. Internal Report. Gdansk University of Technology, 2009.
[13] Nubel K., *Experimental and numerical investigation of shear localization in granular materials*. Publication Series of the Institute of Soil and Rock Mechanics, University of Karlsruhe, 2002.
[14] Ostendorf M., Schwedes J., *Application of Particle Image Velocimetry for velocity measurements during silo discharge*. Powder Technology, 158, 2005, 69–75.
[15] Rechenmacher A.L., Finno R.J., *Digital image correlation to evaluate shear banding in dilative sands*. Geotechnical Testing Journal, 27, 1, 2004, 13–22.
[16] Scott D.M., McCann H., *Process Imaging for automatic control*. Taylor and Francis Group, 439, 2005.
[17] Sideman S., Hijikata K., *Imaging in Transport Processes*. Begell House, 621, 1993.
[18] Słomiński C., Niedostatkiewicz M., Tejchman J., *Application of particle image velocimetry (PIV) for deformation measurement during granular silo flow*. Powder Technology, 173, 1, 2007, 1–18.
[19] Stahzevski S.B., Revushenko A.F., *Localization in granular materials*. Lecture at the Karlsruhe University, 1992.
[20] Tejchman G., Gudehus G., *Verspannung, Scherfugenbildung und Selbsterregung bei der Siloentleerung. In Silobauwerke und ihre spezifischen Beanspruchungen* (eds.: J. Eibl and G. Gudehus). Deutsche Forschungsgemeinschaft, Wiley-VCH, 2000, 245–284.
[21] Vardulakis I., Graf B., Gudehus G., *Trap-door problem with dry sand: a statical approach based upon model test kinematics*. Int. J. Numer. Anal. Meth. Geomech., 5, 57–78, 1981.
[22] White D.J., Randolph M., Thompson B., *An image-based deformation measurement system for the geotechnical centrifuge*. Int. J. Phys. Modell. Geotech., 3, 1–12, 2005.
[23] White D.J., Take W.A., Bolton M.D., *Soil deformation measurements using particle image velocimetry (PIV) and photogrammetry*. Geotechnique, 53, 7, 2003, 619–631.
[24] Yoon J.Y., Patel V.C., *Numerical model of turbulent flow over sand dune*. Journal of Hydraulic Engineering, 122, 1, 1996, 10–18.